Arabian Journal of Chemistry (2023) **16**, 104866

King Saud University

Arabian Journal of Chemistry

www.ksu.edu.sa
www.sciencedirect.com

ORIGINAL ARTICLE

A resorcinarene based chelating agent for selective cloud point extraction of Pb^{2+} ions in water: Synthesis, structural characterization and analytical applications

Jing-Long Liu [a,b], Xin-Min Zhou [a], Meng Sun [a], Ai-Quan Jia [a,*], Hua-Tian Shi [a], Qian-Feng Zhang [a,*]

[a] *Institute of Molecular Engineering and Applied Chemistry, Anhui University of Technology, Ma'anshan, Anhui 243002, PR China*
[b] *Jiangsu Nanjing Environmental Monitoring Center, Nanjing, Jiangsu 210013, PR China*

Received 8 February 2023; accepted 23 March 2023
Available online 29 March 2023

KEYWORDS

Sulfonatomethylated calix[4]resorcinarene;
Chelating agent;
Lead;
Selectivity;
Cloud point extraction;
Inductively coupled plasma atomic emission spectrometry

Abstract A sulfonate-functionalized *C-iso*-butyl-calix[4]resorcinarene was synthesized by the sulfomethylation reaction from calix[4]resorcinarene with formaldehyde solution and sodium sulfite. Sulfonatomethylated calix[4]resorcinarene (C4RS) adopts a symmetrical bowl-shaped conformation in solution and has four methylene sulfonate groups with flexible structure, which provide the possibility of trapping specific metal ions. C4RS is an excellent metal chelating agent and recognizer with good water solubility in the surfactant solution. It is worth noting that C4RS shows selectivity of the Pb^{2+} ion over a variety of other competing metal ions such as Cr^{3+}, Ag^{+}, Cu^{2+}, Co^{2+}, Ni^{2+}, Mn^{2+}, Mg^{2+}, Sb^{3+} and Cd^{2+}. Using C4RS and Trtion X-114 as chelating and extractant agent, respectively, the procedure of cloud point extraction (CPE) could extract Pb^{2+} ion with high efficiency and selectivity. The method of CPE combined with inductively coupled plasma atomic emission spectrometry (ICP-OES) showed low detection limit of 0.0006 mg L^{-1}, high recovery rate and acceptable precision, and could apply to the determination of lead in the tap water and lake water.

* Corresponding authors.
E-mail addresses: jaiquan@ahut.edu.cn (A.-Q. Jia), zhangqf@ahut.edu.cn (Q.-F. Zhang).

Peer review under responsibility of King Saud University.

Production and hosting by Elsevier

https://doi.org/10.1016/j.arabjc.2023.104866
1878-5352

1. Introduction

Calix[4]resorcinarene, as a special subset of calix[4]arene, has been recognized to be a greatly versatile class of supramolecular compound with a bowl-shaped aromatic cavity (Aoyama et al., 1989; Timmerman et al., 1996). Various calix[4]resorcinarene derivatives can be obtained by controlling the type and number of functional groups, among which sulfonatomethylated calix[4]resorcinarene is a typical anionic water-soluble derivative (Kazakova et al., 2000). It is well-known that calix[4]resorcinarenes have attracted extensive attention in various fields such as in supramolecular chemistry (Yamanaka et al., 2011; Ma et al., 2003; Kenji et al., 2003), ions recognition (Lu et al., 2017; Han et al., 2019; Memon et al., 2016; Rustem et al., 2005; Zhang et al., 2020; Larbi et al., 2020), material science (Alina et al., 2017; Shalaeva et al., 2017; Gissawong et al., 2022), and biological science (Ruslan et al., 2018; Ruslan et al., 2020; Janget al., 2018), as versatile host molecules. In recent decades, water-soluble derivative has been widely applied in the recognition of amino acids (Pang et al., 2014; Roberta et al.,2016), alkaloids (Ruslan et al., 2020; Astrid et al., 2019) and anions (Su et al., 2018).

If there is a green, environmentally friendly and convenient process for concentrating and separating to extract metal ions, it must be cloud point extraction (CPE) (Thongsaw et al., 2019; Ulusoy et al., 2012; Sayed et al., 2016). However, an effective chelating agent is necessary to achieve metal recognition with highly selectivity and sensitivity. It is worthy to mention that *p*-sulfonatocalix[4]arene has been successfully synthesized, and used as a metal chelating agent in CPE procedure to achieve selective separation and determination of trace copper(II) from the stock lanthanoid solutions (Asiya et al., 2006; Zairov et al., 2009; Wei et al., 2010). Therefore, sulfonatomethylated calix[4]resorcinarene may also be a potential metal chelating agent with high sensitivity and selectivity to be investigated. Herein, we present synthesis of a *iso*-butyl-substituted sulfonatomethylated calix[4]resorcinarene(C4RS) which is characterized by ^{1}H NMR spectra, Fourier Infrared (FT-IR), powder X-ray diffraction (XRD), and scanning electron microscope with energy dispersive X-ray analyzer (SEM-EDS).

It is well known that lead is one of the most toxic elements in nature, and lead pollution is also very harmful to human health. The US Environmental Protection Agency (EPA) has classified lead as a group B2 (probable) human carcinogen. Based on the chelation of C4RS with metal ions, this work propose an application of C4RS as a complexing agent for selective separation of Pb^{2+} ions based procedure prior to ICP-OES analysis. The goal of the present work is to study the recognition behaviors of Pb^{2+} from mixed metal solutions and the separation and determination of Pb^{2+} with a CPE procedure. The extraction of Pb^{2+} in CPE procedure with C4RS and Triton X-114 (TX114) was examined in detail and the effect of the factors such as pH, the concentrations of TX-114 and C4RS was evaluated. In the present work, a CPE pre-concentration methodology combined with ICP-OES has been developed and optimized for the determination of lead in tap water and lake water based on C4RS.

2. Materials and methods

2.1. Reagents

All solvents used in the experiment were commercial products of high purity and used as received. Sodium sulfite, hydrochloric acid, sodium hydroxide and formaldehyde solution (35%) were purchased from Sinopharm Chemical Reagent Co., Ltd. Triton X-114 was purchased from Shanghai Macklin Biochemical Technology Co., Ltd. The stock solution of metals (1000 mg L^{-1}) was purchased from Institute of Standard Samples of the State Environmental Protection Administration, China. The mixed working solution (1.0 mg L^{-1}) was obtained by mixing ten single stock solution of metals and diluting by serial dilution with 1% (*v*/*v*) HNO_3. *C-iso*-butyl-calix[4] resorcinarene and sulfonatomethylated calix[4]resorcinarene were prepared according to procedures described in the literature (Kazakova et al., 2000; Cram et al., 1988; Liu et al., 2022). All laboratory glassware for trace analysis were treated with 5% (*v*/*v*) HNO_3 for at least 48 h and triplicate rinsed with ultrapure water before use. Metal ions in ultrapure water and all of reagents were not detected.

2.2. Materials characterization

^{1}H NMR spectra were recorded on a NMR spectrometer (Bruker, DPX-400, Switzerland) using tetramethylsilane as internal standard. FT-IR spectra were measured on an FT-IR spectrophotometer (Nicolet, FT 1703X, USA) from 4000 to 400 cm^{-1} region using KBr pellets. Elemental analyses were carried out using a elemental analyzer (Perkin-Elmer, 2400, Shelton, USA). Powder X-ray diffraction (XRD) experiments were recorded on a Bruker D8 Advance (operating at 40 kV and 20 mA) with Ni-filtered Cu-Kα radiation at 1.5406 (Å) with a speed of 0.2 min per step of 0.02° in the range $5° \leq 2\theta \leq 50°$. The surface microstructures were investigated under a scanning electron microscope (SEM, JEOL JSM-6490LV, Japan) with an energy dispersive X-ray analyzer. UV–visible spectra were recorded on a TU1900 spectrophotometer (Beijing Purkinje General, China) equipped with UVWin 6.0.0 software, using a 0.1 cm path-length cell.

2.3. CPE procedure and ICP-OES analysis

In 50 mL graduated plastic centrifuge tubes, a certain volume of metal standard solution, 1.0 g L^{-1} C4RS solution, 5% (*v*/*v*)

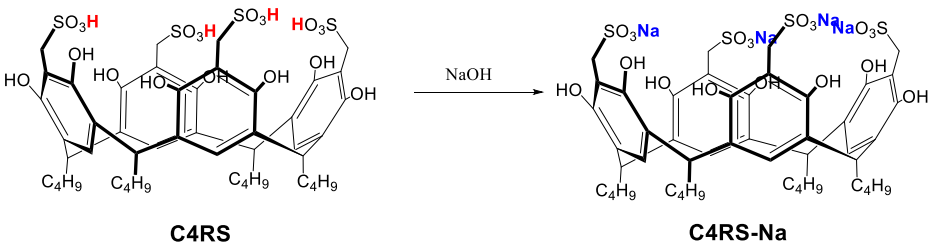

Scheme 1 Synthetic procedures of C4RS-Na.

TX114 solution and 2 mL Britton-Robinson buffer solution were added, and then the total volume was made up to 50 mL with ultrapure water. The solution was heated with ultrasonic treatment in 50 °C for 10 min, then centrifuged for 10 min at 3000 rpm and finally kept in an ice-bath for several minutes. The heavier surfactant-rich phase became viscous and settled to the bottom. The supernatant aqueous phase was carefully removed with a pipette. The process of CPE was shown in Fig. 1. And the lower surfactant-rich phase was diluted to 5 mL with 5% (*v*/*v*) HNO_3 after the addition of 0.4 mL tributyl phosphate solution, followed by an inductively coupled plasma optical emission spectrometer (ICP-OES) analysis (Sounderajan et al., 2010; Souz et al., 2020; Guillaume et al., 2018).

The inductively coupled plasma atomic emission spectrometry (ICP-OES) (PerkinElmer, Optima 8300, Shelton, USA) was used for all determinations of lead (Pb I 220.353 nm), chromium (Cr I 267.716 nm), silver (Ag I 328.068 nm), copper (Cu I 327.393 nm), cobalt (Co I 228.616 nm), nickel (Ni I 231.604 nm), manganese (Mn I 285.213 nm), magnesium (Mg I 220.353 nm), antimony (As I 220.353 nm) and cadmium (Cd I 340.4 nm). The ICP-OES configuration and operation conditions include 40 MHz of generating frequency and 1300 W of radiofrequency power. The argon gas flow rate was 15.0 L min^{-1} for plasma formation, 0.30 L min^{-1} for auxiliary gas, and 0.55 L min^{-1} for nebulising gas. The measurements were made in triplicate, with 10 s of read time and while viewing axially. The sample introduction system consisted of a concentric nebuliser and a cyclonic spray chamber.

3. Results and discussion

3.1. Synthesis and characterization

Sulfonatomethylated calix[4]resorcinarene was synthesized by sulfonation of *C-iso*-butylcalix[4]resorcinarene with sodium sulfite in the presence of excess formaldehyde in the solution of water and in a high yield (90%∼98%). C4RS is insoluble in common organic solvents such as chloroform, methylene chloride, acetone, 1,4-dioxane, toluene, ethyl acetate, *N*,*N*-dimethylformamide (DMF), but it has a good solubility in water and form C4RS-Na in basic medium aqueous. C4RS-Na was prepared by adding NaOH solution to C4RS solution and deprotonating it (Scheme 1). Then, the pure sample of C4RS-Na was obtained by adding ethanol to recrystallization, and the formation of the C4RS-Na sample was determined by elemental analysis (Anal. Calc. for C4RS-Na: C 48.97, H 5.14, O 27.18, S 10.90; found: C 46.22, H 5.31, O 28.66, S 9.88).

The chemical structure of C4RS was confirmed by ^{1}H NMR (Fig. 2). The peaks at 7.33 ppm (s, 4H) is related to the four equivalent benzene protons, indicating that C4RS adopts a symmetrical (C_{4v}) bowl-shaped conformation. The bridging methine protons in C4RS appeared at around 4.36–4.41 ppm as a triplet, while the protons of the Ar-CH_2-S groups are easily identified as a singlet at about 3.88 ppm (Kazakova et al., 2000; Edilma et al., 2015; Twum et al., 2020). Especially, C4RS maintains the peaks of partial protons on the hydroxyl groups in solution at 9.74 ppm.

In order to further verify the complexation of C4RS with Pb^{2+} ion, the structure of C4RS and C4RS-Pb were also characterized by Fourier-transform infrared (FT-IR) spectroscopy (Fig. 3). The FT-IR spectra of C4RS and C4RS-Pb show the absorption band of hydroxyl groups (Ar-OH) at about 3421 cm^{-1} and intense absorption bands of stretching vibrations of the aromatic ring at 1603 cm^{-1} and 1461 cm^{-1}. The peaks at around 1050 cm^{-1} and 770 cm^{-1} ascribed to the S = O and S–O bonds. The FT-IR spectrum of C4RS shows the stretching vibrational absorption band of sulfonate groups –SO_2OH at about 1347 cm^{-1}. However, the FT-IR spectrum of C4RS-Pb shows a weak absorption at 1347 cm^{-1} and an absorption band of –SO_2OH-M^+ at about 1133 cm^{-1} (Edilma et al., 2015; Twum et al., 2020). According to reports in the literature (Milena et al., 2014; Liu et al., 2022), we can speculate that lead ions can have strong coordination with sul-

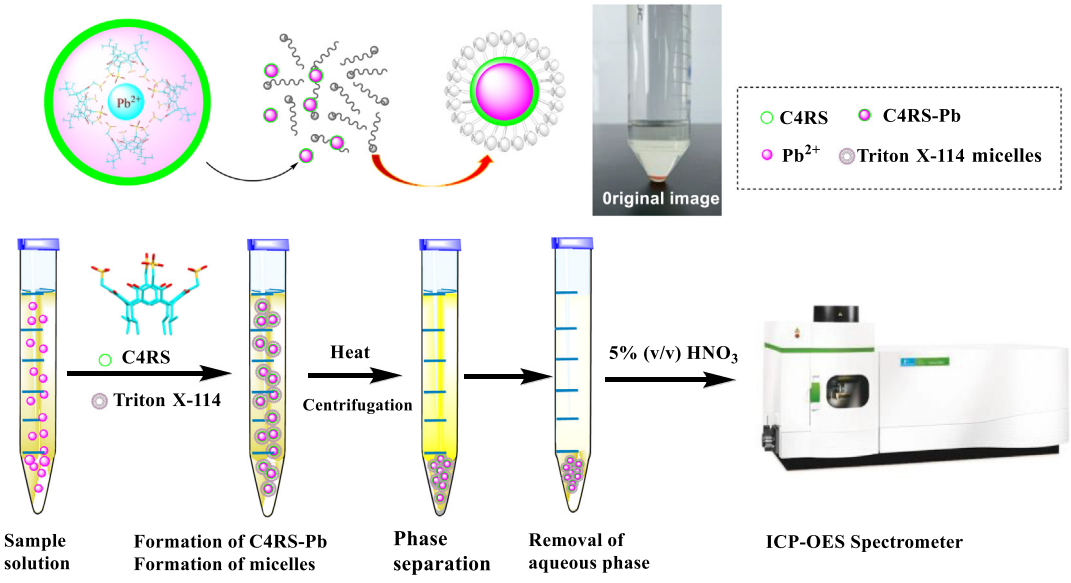

Fig. 1 The procedure of cloud point extraction.

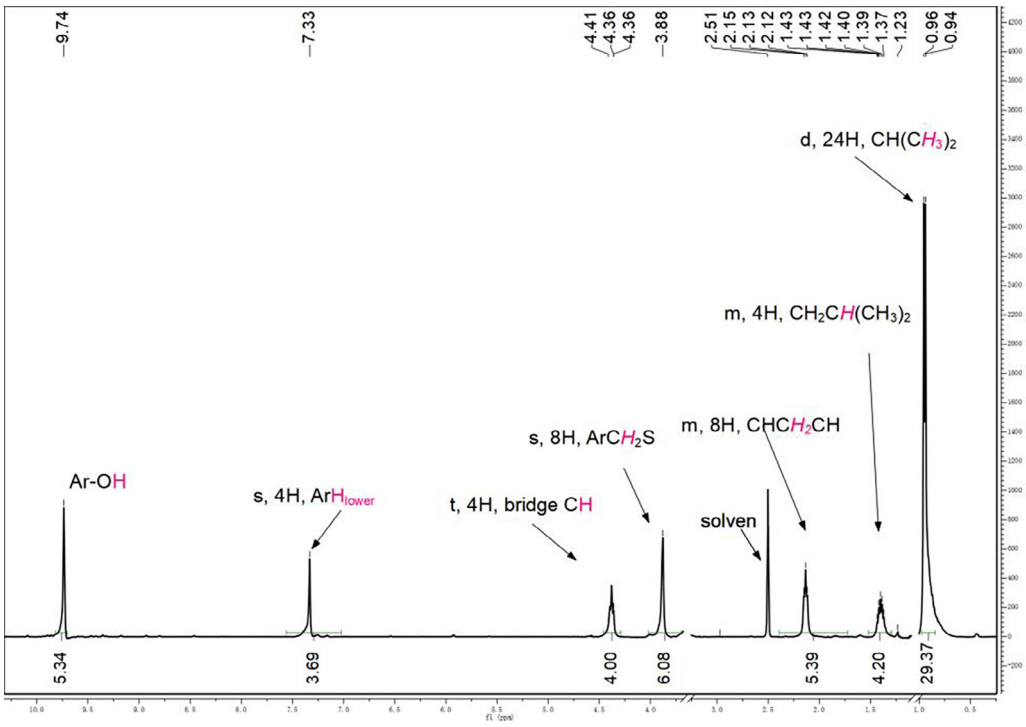

Fig. 2 ^{1}H NMR spectrum of C4RS (The assignments of the signals were indicated).

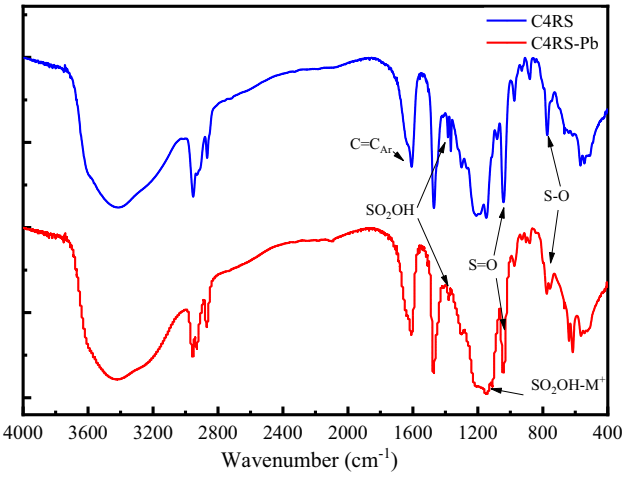

Fig. 3 FT-IR spectra of C4RS and C4RS-Pb.

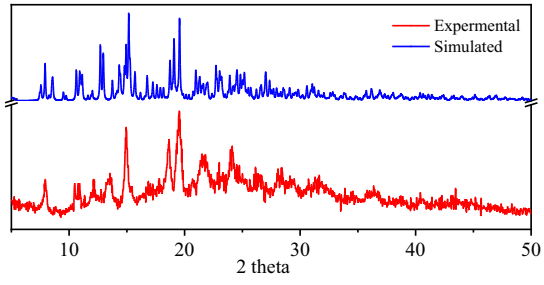

Fig. 4 The simulated and experimental PXRD of C4RS-Na.

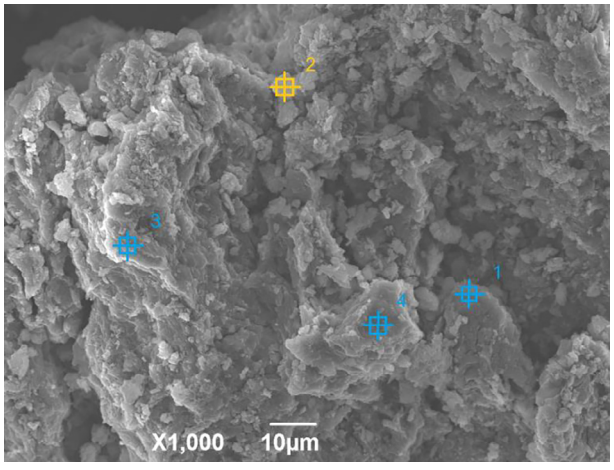

Fig. 5 SEM image of C4RS-Na.

fonic acid groups in C4RS. In the aqueous solution, Pb^{2+} may bond with the oxygen atoms from several water ligands and sulfonate groups from C4RS units.

The phase purity of the as-synthesized products of C4RS-Na were verified by the simulated and experimental powder X-ray diffractometry patterns, as shown in Fig. 4. The simulated XRD patterns were calculated from single-crystal data in our previous paper (Liu et al., 2022), which compared with the patterns obtained from the the bulk power solid samples of C4RS-Na. Nearly all reflections of the measured pattern correspond to the simulation, indicating the phase purity of the C4RS-Na samples. To understand the surface morphologies of C4RS-Na, the microstructures were investigated by scan-

ning electron microscopy (SEM) as shown in Fig. 5. The SEM image of C4RS-Na reveals the amorphous morphology composed of the large assembly of particles. The corresponding EDS results of site 1–4 are summarized in Table 1, which were principally correspond to the theoretical calculation.

3.2. UV–vis spectroscopy and quantitative analysis

To verify the quantitative binding ability of C4RS and Pb^{2+}, the UV–vis absorption spectra of C4RS and a series of lead standard solutions were analyzed. Using water and C4RS as reference solutions respectively, a series of UV–vis spectra were obtained (Kashapov et al., 2015; Liu et al., 2020). With the addition of Pb^{2+} ion, the absorption intensity of UV–vis absorption gradually increases and the maximum absorption wavelength exhibited a bathochromic shift from 287 nm to 296 nm, as shown in Fig. 6(a). It is clearer that C4RS-Pb complex has maximum characteristic absorption at 302 nm when C4RS solution was used as reference solution, shown in Fig. 6(b). In addition, the relative absorbance of C4RS-Pb at 302 nm shows a good linear relationship with the concentration of Pb^{2+} ions in the range of 0.02–0.64 mg L^{-1}, with r = 0.9996, shown in Fig. 6(c). The linear regression equation was $A_{302nm} - A_{(C4RS,\ 302\ nm)} = 1.426[Pb^{2+}] + 0.0007$, where $[Pb^{2+}]$ was the mass concentration (mg L^{-1}) of Pb^{2+}, A_{302nm} was the absorbance of C4RS-Pb at 302 nm, and $A_{(C4RS,302\ nm)}$ was the absorbance of C4RS without of Pb^{2+} at 302 nm.

Table 1 Semi-quantitative EDS results for site 1 ~ 4 in Fig. 5.

Element (wt. %)	C	O	Na	S	Other
site 1	49.33	31.22	7.20	5.67	6.58
site 2	49.10	31.10	6.68	4.64	8.48
site 3	51.61	27.98	6.92	5.68	7.81
site 4	49.37	30.03	6.19	6.37	8.04
theoretical calculation	48.97	27.18	7.81	10.89	5.15

3.3. Optimum extraction conditions

Take metal ions mixed standard solution (Pb^{2+}, Cr^{3+}, Ag^{+}, Cu^{2+}, Co^{2+}, Ni^{2+}, Mn^{2+}, Mg^{2+}, Sb^{3+}, Cd^{2+}) with a concentration (1.0 mg L^{-1}) into a 50 mL centrifuge tube and then the total volume was made up to 50 mL with ultrapure water. After adding C4RS solution and surfactant TX114 solution, the pH was adjusted, and the cloud point extraction (CPE) procedure was carried out for the mixed metal solution. In order to explore the optimum extraction conditions for

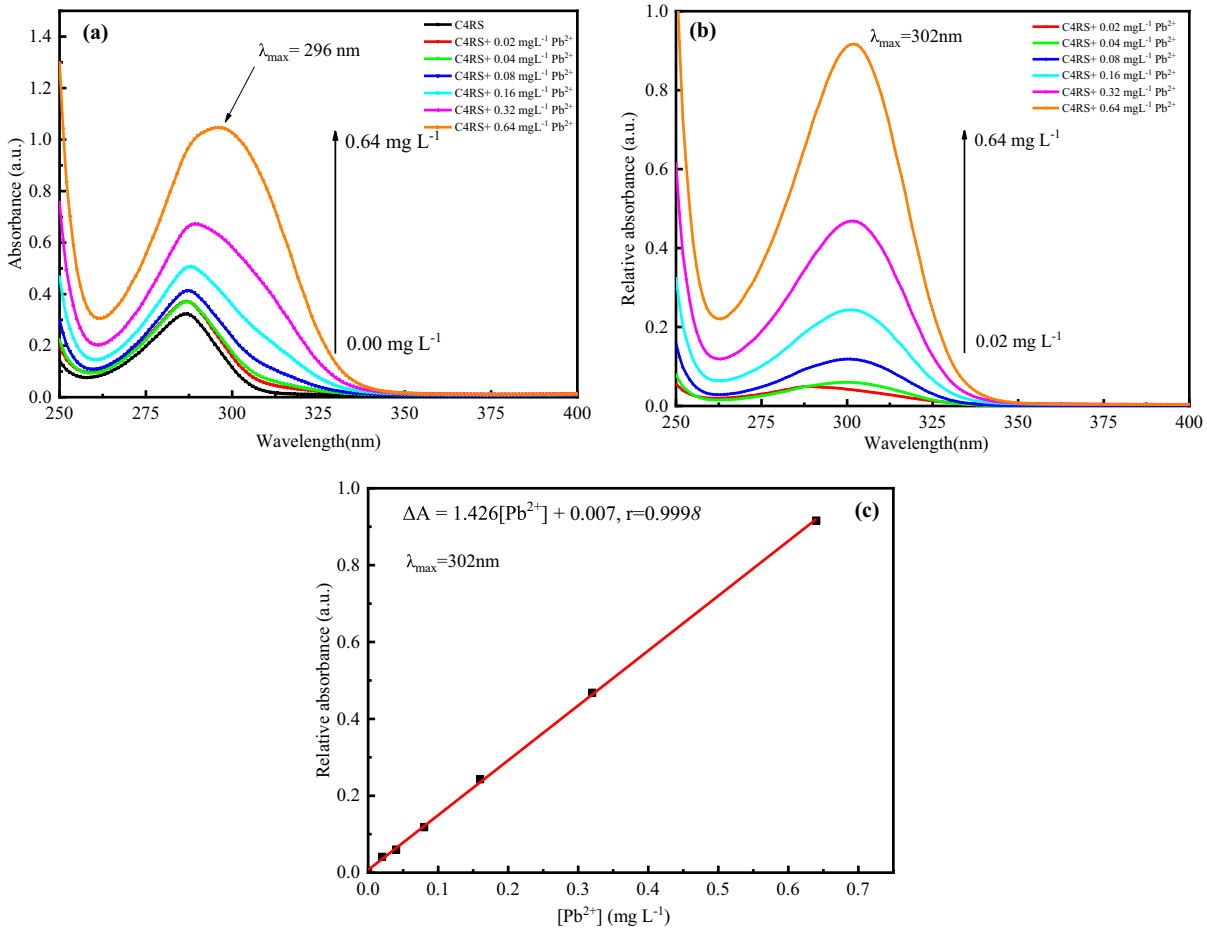

Fig. 6 UV–vis spectra of CSRS in aqueous solutions of Pb^{2+} with different concentrations.

extracting metal ions by C4RS, the most suitable conditions of pH, C4RS and TX114 concentration, extraction temperature and time were investigated. The content of mixed metal ions in the surfactant phase after extraction was simultaneously determined by ICP-OES. The extraction efficiency was calculated by spiked recovery rate in the following discussion of results.

3.3.1. Effect of pH on CPE.

In the process of CPE, pH plays an important role in the formation and chemical stability of metal-chelate (Mortada et al., 2020). It is well known that the deprotonation of C4RS depends on the acidity of the solution, which heavy metal ions to different coordination ability of C4RS toward the metals. However, metal ions will precipitate or oxide in alkaline solutions, which cannot be extracted, while hydrophobic complexes cannot be formed in strongly acidic solutions. In addition, it has been reported in literature that the neutral form of chelate could interact with the micellar aggregate strongly than its ionic form (Frankewich et al., 1994).

As shown in Fig. 7, it can be seen that the extraction efficiency of all metal ions is low in the range of pH 1–5, and the selectivity of Ag^+ ion is significantly higher than other ions in pH the range of 3–5. The extraction system showed high extraction efficiency and selectivity for Pb^{2+} and Cr^{3+} ions higher at pH 7. It indicates that C4RS has stronger coordination ability with Pb^{2+} and Cr^{3+} ions than other ions under neutral conditions, and the hydrophobic association could be effectively extracted into micellar phase than ionic association (Asiya et al., 2006). The extraction efficiencies of Pb^{2+} and Cr^{3+} ions were 99.9% and 80.3%, respectively. C4RS was basically deprotonated at pH $>$ 7 and more metal ions bind to C4RS and extracted into the surfactant phase, such as Pb^{2+}, Cr^{3+}, Cu^{2+}, Mn^{2+}, Ni^{2+}, Co^{2+} and Cd^{2+}. When the pH = 8, more kinds of metal ions can be combined by C4RS, and mutual interference is enhanced, resulting in false positives. Therefore, under neutral conditions, the selectivity of lead ions can be improved to reduce the interference of other ions. However, with the increase of alkalinity of the solution, the selectivity of C4RS to metal ions decreases, and the extraction efficiency of all ions except Sb^{3+} tended to be uniform. It can be concluded that C4RS/TX114 extraction system can selectively extract Pb^{2+} and Cr^{3+} ions under neutral conditions, and has a especially high extraction efficiency for Pb^{2+}. Therefore, all the following experiments were carried out at pH 7.

3.3.2. Effect of TX114 dosage on CPE

TX114 and C4RS were used as extractant and chelating agent to complete the identification and extraction of metal ions, respectively. C4RS and TX114 have good mutual solubility in H_2O, which is a double-edged sword. In other words, TX114 can improve the solubility of C4RS in solution, but good intersolubility will increase the temperature of cloud point and even cause the disappearance of cloud point phenomenon. Therefore, it is necessary to study the optimal dosage of chelating agent and extractant and improve their synergistic effect. The extraction of the metals with TX114 being in the range of 0.2–2.5 mL was investigated, as shown in Fig. 8. It can be seen from the results that the concentration of TX114 is too low to completely extract metal chelates, but not the more the better. Because the high concentration of surfactant will make the viscosity of the extraction liquid increase and reduce the atomization efficiency of ICP-OES to affect the determination results. When the dosage of TX114 solution is 1.2–1.5 mL, the extraction efficiency of Pb^{2+} and Cr^{3+} ions could reach 88.0%–99.9% and 62.5%–80.3%, which is significantly higher than that of other ions, showing good selectivity for Pb^{2+}. Further investigations were carried out in the presence of 1.5 mL of TX114 solution.

3.3.3. Effect of C4RS dosage on CPE

The effect of C4RS concentration on the extraction of metal ions was studied in the range of 0.2–2.0 mL and the results were illustrated in Fig. 9. Generally speaking, the larger the amount of chelating agents, the more complete the binding

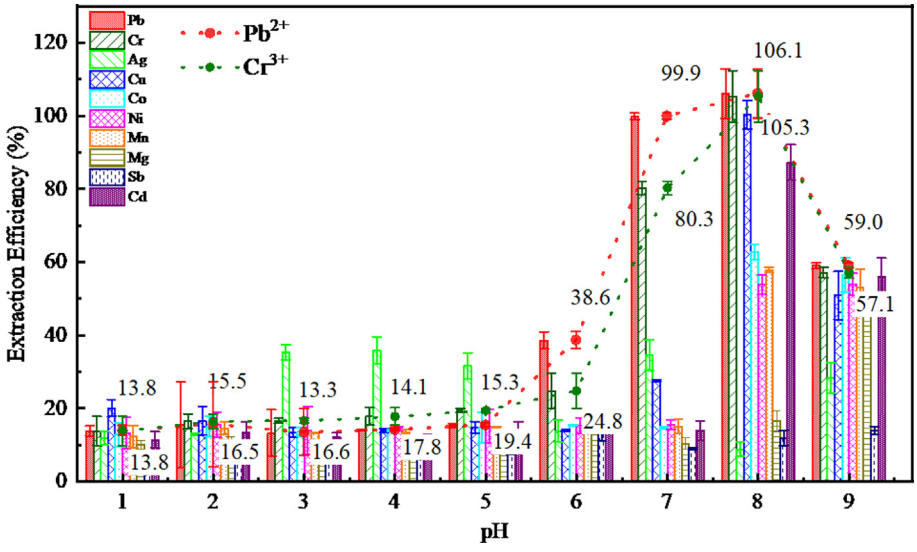

Fig. 7 Effect of pH on the extraction of metal ions represented as bar graphs; Pb^{2+} and Cr^{3+} were also specially shown as dot plots. pH 1, 2, 3, 4, 5, 6, 7, 8, 9; C4RS: 0.03 mmol L^{-1}, 1.5 mL; Triton X-114: 0.15 % (v/v). The error bars standard for"± one standard deviation of three trials".

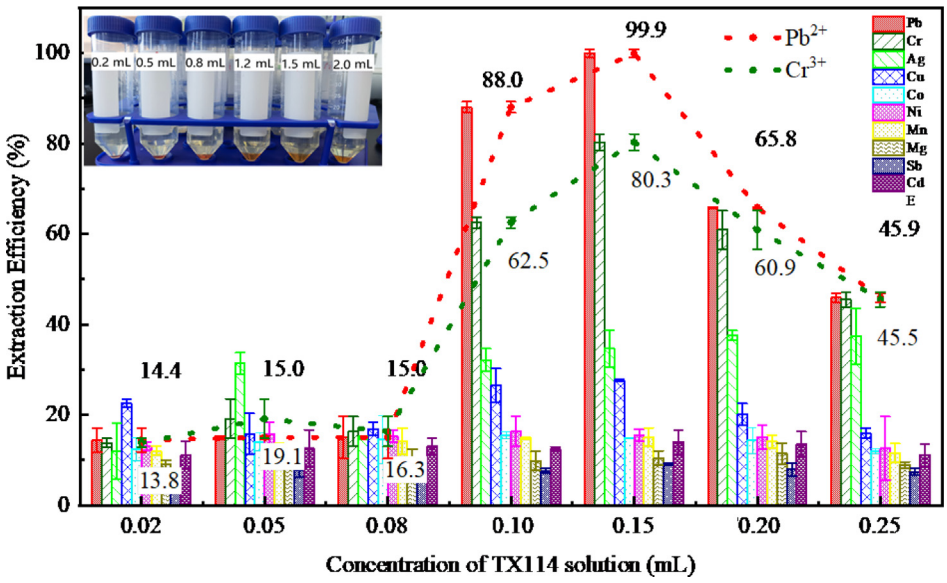

Fig. 8 Effect of TX114 on the extraction of metal ions represented as bar graphs; Pb^{2+} and Cr^{3+} were also specially shown as dot plots (The inset photograph in the figure shows the separation at different dosage of TX114). pH 7; C4RS, 0.03 mmol/L; Triton X-114 solution concentration (%, *v*/*v*), 0.02,0.05, 0.08, 0.12, 0.15, 0.20, 0.25.

of metal ions. However, in the process of CPE, the chelating agents and extractants synergistically interact and influence each other. As the concentration of C4RS increases, on the one hand, the cloud point of the surfactant is not obvious or not generated in the extraction process; on the other hand, when C4RS reaching a concentration value, it forms hydrophilic complex with the metal ions, which cannot be extracted by the surfactant. When the dosage of C4RS solution is 0.8–1.5 mL, the extraction efficiency of Pb^{2+} and Cr^{3+} ions can reach 85.6%–102% and 68.0%–80.3%.

3.3.4. Equilibrium temperature and time

In order to obtain the lowest equilibrium temperature and the shortest equilibrium time in the extraction process, the effects of equilibrium temperature and time on extraction efficiency of Pb^{2+} ion were studied in the range of 20–80 °C and 5–30 min, as shown in Fig. 10. In this experiment, ultrasonic water bath was used for extraction balance, and the extraction was completed in the shortest time and at a lower equilibrium temperature. The results show that the extraction efficiency is higher when the equilibrium temperature is above 50 °C, but it does

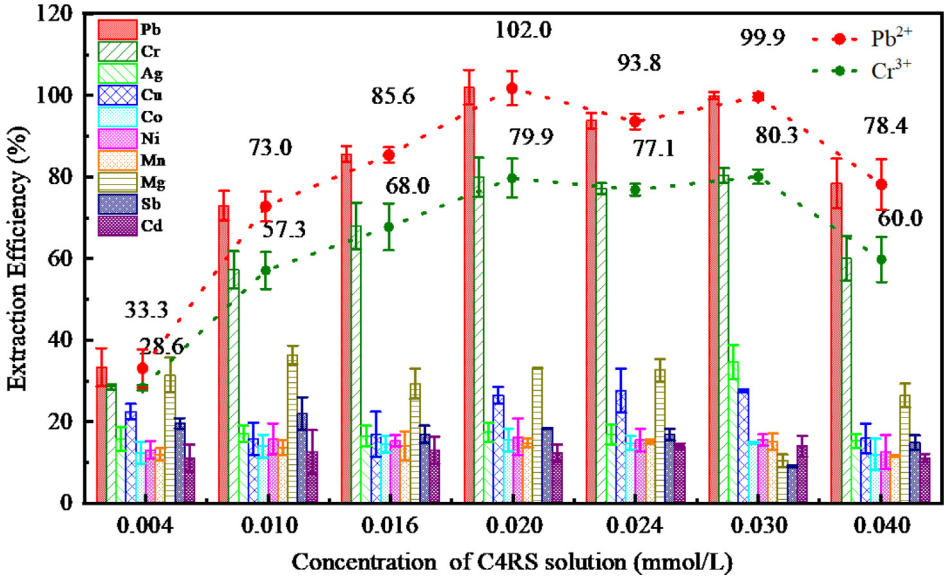

Fig. 9 Effect of C4RS on the extraction of metal ions represented as bar graphs; Pb^{2+} and Cr^{3+} were also specially shown as dot plots. pH 7; C4RS, 0.004, 0.010, 0.016, 0020, 0.024, 0.030, 0.040 mmol/L; Triton X-114, 0.15 % (v/v).

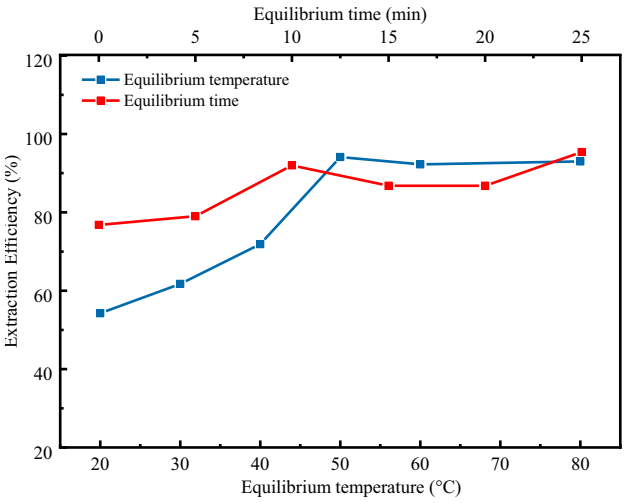

Fig. 10 Effect of equilibrium temperature and time on the extraction of Pb^{2+} ions.

not increase with the temperature increasing. At a tiny ultrasonic frequency, the micelles can more quickly and fully capture hydrophobic chelates compared with non-ultrasound-assisted extraction. However, ultrasound assisted extraction can not reduce the cloud point temperature. Ultrasonic assistance can shorten the balancing time and complete the extraction balancing process within 10 min. But the longer ultrasonic time will damage the micelles and reduce the extraction efficiency.

3.3.5. Antifoam agent

The surfactant will produces heavy foams during atomization, which affect the stability of the signal and damage the equipment. Therefore, the addition of antifoam agent to the surfactantrich phase before determination for eliminating the influence of surfactants. So, the tributyl phosphate used as antifoam agent in this case. The tributyl phosphate needed to be diluted by ethanol before use due to its large viscosity. Further study showed that 0.4 mL of 50% (v/v) tributyl phosphate ethanol solution could significantly suppress surfactant foaming.

Based on the above experimental results, the extraction efficiency of Pb^{2+} is the highest, and far higher than that of other metal ions. The reasonable explanation might be that the hydrophobic compounds formed by C4RS and Pb^{2+}, which extracted into micellar pseudo-phase much more efficiently than ionic associates formed by other ions.

3.4. Method evaluation

Under the optimized experimental conditions, the limits of detection, precision and accuracy of the method were taken as the characteristic indexes to investigate the analytical performance of this method for 50 mL samples. Under the operating parameters of ICP-OES, the concentrations of Pb^{2+} were linearly related to the emission intensity values in the range of 0.1–2.0 mg/L, with correlation coefficients better than 0.999.

3.4.1. Limit of detection and quantification (LOD and LOQ)

As no lead was detected in the blank sample experiment, the LOD was determined by the spiked sample. 1.0 mL of the lead standard solution of 1.0 mg L^{-1} was added in a 50 mL centrifuge tube, and the pH was adjusted to 7 buffer solution before making the total volume up to 50 mL with ultrapure water. Eleven samples with a concentration of 0.02 mg L^{-1} Pb^{2+} were prepared by this method. According CPE procedure, C4RS solution and TX-114 solution were successively added. The samples were tested by ICP-OES after CPE. The results of the eleven samples were shown in Table 2. The method detection limit for determination of Pb^{2+} was studied under the optimal experimental conditions of CPE. The LOD and LOQ were obtained from LOD = 3σ and LOD = 10σ, σ stands for standard deviation (SD). The LOD and LOQ could reach 0.0006 mg L^{-1} and 0.002 mg L^{-1}. The LOD could below actual maximum acceptable concentration for Pb in the drinking water by WHO and China (0.010 mg L^{-1}).

3.4.2. Precision and accuracy of method

According to the CPE procedure, the spiked samples with concentrations of 0.05, 0.10 and 0.12 mg L^{-1} were preprocessed and then tested by ICP-OES. The relative standard deviations (RSD) of the three spiked samples were 5.3%, 4.4% and 2.6% (n = 6), with excellent spiked recoveries of 98.1%, 101% and 101% respectively, indicating that the method has good accuracy, as shown in Table 3.

Table 2 Analytical results of the spiked sample (n = 11).

Concentration (mg L^{-1})						Mean (mg L^{-1})	σ (mg L^{-1})	MDL (mg L^{-1})
0.0176	0.0180	0.0176	0.0178	0.0177	0.0175	0.0177	0.0002	0.0006
0.0172	0.0176	0.0180	0.0178	0.0175				

Table 3 Analytical results of precision and accuracy (n = 6).

	Concentration after CPE (mg L^{-1})			Mean (mg L^{-1})	Spiked (mg L^{-1})	RSD (%)	Recovery (%)
Spiked sample 1	0.523	0.477	0.474	0.505	0.50	5.3	101
	0.536	0.527	0.494				
Spiked sample 2	1.033	0.939	0.998	1.012	1.00	4.4	101
	1.030	0.264	0.303				
Spiked sample 3	1.135	1.149	1.197	1.179	1.20	2.6	98.1
	1.212	1.200	1.179				

Table 4 Analytical results for detection of lead in water samples.

	Concentration (mean, $n = 3$) (mg L^{-1})			
	Pb^{2+} added	Pb^{2+} found	RSD(%)	Recovery (%)
Tap water 1	0.0	ND[a]	1.1	–
	0.020	0.0177 ± 0.0020[b]		88.5
Tap water 2	0.0	ND	1.4	–
	0.020	0.0175 ± 0.0025		87.5
Lake water 1	0.0	ND	1.4	–
	0.020	0.0180 ± 0.0025		90.0
Lake water 2	0.0	ND	2.5	–
	0.020	0.0189 ± 0.0047		94.5

[a] Not detected.
[b] Mean ± SD (n = 3).

Table 5 Comparison of the reported methods with the proposed method.

Enrichment method	Detection method	RSD(%)	Detection limit (mg L^{-1})	Ref.
CPE	FAAS[c]	1.6–3.2	0.0045	Silva and Roldan (2009)
CPE	ICP-OES	11	0.04	Jolanta et al. (2010)
CPE	ICP-OES	6.0	0.00034	Zhao et al. (2012)
CPE	FAAS[c]	4.9	0.0043	Wen et al. (2012)
CPE	FAAS	1.6	0.005	Sayed et al. (2016)
CPE	ICP-OES	/	0.0008	Guillaume et al. (2018)
CPE	ICP-OES	1.1–2.5	0.0006	This work

[c] FAAS: Flame atomic absorption spectrometry.

3.4.3. Determination of selenium in real samples

In order to investigate the applicability of this method to the analysis of lead content in real water samples, the lake water and tap water samples were analyzed and evaluated. The lake water and tap water filtered by 0.45 μm membrane and acidified were pretreatment according to the optimal CPE conditions, and the enrichment factor was 10. Due to preconcentration treatment by CPE, the sensitivity of lead determination in water is obviously improved. The lead was not observed in the two tap water and two lake water samples. The recoveries were between 87.5% and 94.5% by spiking the standard at 0.02 mg L^{-1} with RSDs (1.1%–2.5%), as shown in Table 4. Thus, the proposed CPE-ICP-OES method was effective and reliable for determination of lead in real water samples.(See Table 5).

4. Conclusions

In conclusion, a sulfonate-functionalized *C-iso*-butyl-calix[4] resorcinarene with four flexible methylene sulfonate sites was synthesized by the condensation reaction from calix[4]resorcinarene with formaldehyde solution and sodium sulfite in a quantitative yield. The structure of the obtained C4RS was characterized by NMR, FT-IR, PXRD, and SEM-EDS. The quantitative relationship between C4RS and Pb^{2+} ion was determined by UV–vis spectroscopy, and the absorbance of C4RS-Pb was proportional to Pb^{2+} ion concentration. Under the condition of pH 7, through selecting the appropriate concentration of C4RS and TX114, Pb^{2+} could be extracted by cloud point extraction with high efficiency and selectivity from mixed metal solution, especially the lead extraction efficiency could be up to 99.9%. It had been demonstrated that this CPE procedure system was efficient in neutral condition and could also be coupled with ICP-OES for sensitive analysis of lead. Under optimum experimental conditions, the method gave a low LOD of 0.0006 mg L^{-1}, the relative standard deviations were 2.6% to 5.3%, and the recoveries varied between 98.1% and 101% depending on the spiked samples of pure water and 87.5% to 94.5% depending on the spiked samples of real water samples. The method could be applied to the determination of lead in water samples.

Declaration of Competing Interest

The authors declare that they have no known competing financial interests or personal relationships that could have appeared to influence the work reported in this paper.

Acknowledgements

This project was supported by National Natural Science Foundation of China (90922008) and the Natural Science Foundation of Universities of Anhui Province (KJ2019A0060).

References

Alina, M.E., Julia, E.M., Yana, V.S., Victor, V.S., Irek, R.N., Marsil, K.K., Igor, S.A., Alexander, I.K., 2017. The supramolecular approach to the phase transfer of carboxylic calixresorcinarene-capped silver nanoparticles. Colloid. Surf. A 524, 127–134. https://doi.org/10.1016/j.colsurfa.2017.04.045.

Aoyama, Y., Tanaka, Y., Sugahara, S., 1989. Molecular recognition. 5. molecular recognition of sugars via hydrogen-bonding interaction with a synthetic polyhydroxy macrocycle. J. Am. Chem. Soc. 111 (14), 5397–5404. https://doi.org/10.1021/ja00196a052.

Asiya, M., Julia, E., Alexander, B., Irina, K., Rustem, Z., Rustem, A., Svetlana, S., Alexander, K., 2006. Cloud point extraction of lanthanide(III) ions via use of Triton X-100 without and with

water-soluble calixarenes as added chelating agents. Talanta 68, 863–868. https://doi.org/10.1016/j.talanta.2005.06.011.

Astrid, V.-S., Roger, S.F., Edilma, S., Adrián, P.-R., Mauricio, M., 2019. Host-guest inclusion systems of tetra(alkyl)resorcin [4]arenes with choline in DMSO: Dynamic NMR studies and X-ray structural characterization of the 1:1 inclusion complex. J. Mol. Struct. 1198, (15). https://doi.org/10.1016/j.molstruc.2019.07.093 126846.

Cram, D.J., Karbach, S., Kim, H.E., Knobler, C.B., Maverick, E.F., Ericson, J.L., Helgeson, R.C., 1988. Host-guest complexation. 46. cavitands as open molecular vessels form solvates. J. Am. Chem. Soc. 110 (7), 2229–2237. https://doi.org/10.1021/ja00215a037.

Edilma, S., Miguel, Á.E., Adrián, P.-R., Edgar, V., Mauricio, M., 2015. Synthesis and characterization of two sulfonated resorcinarenes: a new example of a linear array of sodium centers and macrocycles. Molecules 20, 9915–9928. https://doi.org/10.3390/molecules20069915.

Frankewich, R.P., Hinze, W.L., 1994. Evaluation and optimization of the factors affecting nonionic surfactant-mediated phase separations. Anal. Chem. 66, 944–954. https://doi.org/10.1021/ac00079a005.

Gissawong, N., Srijaranai, S., Nanan, S., Kanit, M., Pikaned, U., Norio, T., Siriboon, M., 2022. Electrochemical detection of methyl parathion using calix[6]arene/bismuth ferrite/multiwall carbon nanotube-modified fluorine-doped tin oxide electrode. Microchim. Acta 189, 461. https://doi.org/10.1007/s00604-022-05562-5.

Guillaume, B.C., Dominic, L., Determination of Pb in environmental samples after cloud point extraction using crown ether. Talanta 179, 300−306. https://doi.org/10.1016/j.talanta.2017.11.015.

Han, X., Yang, J., Liu, Y.Y., Ma, J.-F., 2019. Nine coordination polymers assembled with a novel resorcin[4]arene tetracarboxylic acid: selective luminescent sensing of acetone and Fe^{3+} ion. Dyes Pigments 160, 492–500. https://doi.org/10.1016/j.dyepig.2018.08.041.

Jang, Y.-M., Yu, C.J., Kim, J.S., Kim, S.-U., 2018. Ab initio design of drug carriers for zoledronate guest molecule using phosphonated and sulfonated calix[4]arene and calix[4]resorcinarene host molecules. J. Mater. Sci. 53, 5125–5139. https://doi.org/10.1007/s10853-017-1930-8.

Jolanta, B.-B., Anna, S.-M., Wiesław, Ż., 2010. Determination of toxic and other trace elements in calcium-rich materials using cloud point extraction and inductively coupled plasma emission spectrometry. J. Hazard. Mater. 182, 477–483. https://doi.org/10.1016/j.jhazmat.2010.06.057.

Kashapov, R.R., Zakharova, L.Y., Saifutdinova, M.N., Kochergin, Y. S., Gavrilova, E.L., Sinyashin, O.G., 2015. Construction of a water-soluble form of amino acid C-methylcalix[4]resorcinarene. J. Mol. Liq. 208, 58–62. https://doi.org/10.1016/j.molliq.2015.04.025.

Kazakova, E.K., Makarova, N.A., Ziganshina., A.U., Liya, A.M., Abdurakhim, A.M., Wolf D.H., 2000. Novel water-soluble tetrasulfonatomethylcalix[4]resorcinarenes. Tetrahedron Lett. 41(51), 10111–10115. https://doi.org/10.1016/S0040-4039(00)01798-6

Kenji, K., Kei, I., Shigeru, S., Toshiaki, S., Kentaro, Y., 2003. Guest-induced assembly of tetracarboxyl-cavitand and tetra(3-pyridyl)-cavitand into a heterodimeric capsule via hydrogen bonds and CH-halogen and/or CH-π interaction: control of the orientation of the encapsulated guest. J. Am. Chem. Soc. 125 (35), 10615–10624. https://doi.org/10.1021/ja035337q.

Larbi, E., Abdul, S., Judit, T., István, S., 2020. A piezogravimetric sensor platform for sensitive detection of lead (II) ions in water based on calix[4]resorcinarene macrocycles: Synthesis, characterization and detection. Arab. J. Chem. 13, 4448–4461. https://doi.org/10.1016/j.arabjc.2019.09.002.

Liu, X.-L., Liu, J.-L., Wang, N.-N., Jia, A.-Q., Zhang, Q.-F., 2020. Syntheses and structures of thiophosphorylatocavitands and their reactivity towards first-row transition metal halides. Inorg. Nano-Met. Chem. 50, 1315–1321. https://doi.org/10.1080/24701556.2020.1749073.

Liu, J.L., Zhang, P.Z., Jia, A.Q., Shi, H.T., Zhang, Q.F., 2022. Supramolecular assemblies of sulfonatomethylated calix[4]resorcinarenes with aquated sodium(I), cesium(I), and aluminum(III) ions. ChemistrySelect 7, e202104118.

Lu, B.B., Jiang, W., Yang, J., Liu, Y.-Y., Ma, J.-F., 2017. Resorcin[4]arene-based microporous metal-organic framework as an efficient catalyst for CO_2 cycloaddition with epoxides and highly selective luminescent sensing of $Cr_2O_2^{7}$. ACS Appl. Mater. Interfaces. 9 (45), 39441–39449. https://doi.org/10.1021/acsami.7b14179.

Ma, B.Q., Zhang, Y., Coppens, P., 2003. Multiple conformations of benzil in resorcinarene-based supramolecular host matrixes. J. Org. Chem. 68, 9467–9472. https://doi.org/10.1021/jo035169k.

Memon, S., Bhatti, A.A., Bhatti, A.A., Ocak, Ü., Ocak, M., 2016. Calix[4]arene based dual fluorescent sensor for Al^{3+} and $S_2O_7^{2-}$. J. Fluoresc. 26, 1591–1599. https://doi.org/10.1007/s10895-016-1843-y.

Milena, Đ., Dejan, J., Goran, N.K., Santiago, G.-R., Boban, A., Dušanka, R., Ilija, B., 2014. Synthesis and spectroscopic properties of large single-crystals of Pb(II), Hg(II) and Sr(II) methanesulfonato 1D coordination polymers. Polyhedron. 80, 282–289. https://doi.org/10.1016/j.poly.2014.05.056.

Mortada, W.I., 2020. Recent developments and applications of cloud point extraction: a critical review. Microchem. J. 157,. https://doi.org/10.1016/j.microc.2020.105055 105055.

Pang, T.-T., Liu, H.-L., Du, L.-M., Chang, Y.-X., Fu, Y.-L., 2014. Supramolecular interaction of two tryptophans with p-sulfonated calix[4,6,8]arene. J. Fluorese. 24, 143–152. https://doi.org/10.1007/s10895-013-1280-0.

Roberta, P., Giovanna, B., Alessandro, P., Daniela, M., Daniel, H., Pablo, B., Silvano, G., Enrico, D., 2016. The origin of selectivity in the complexation of N-methyl amino acids by Tetraphosphonate Cavitands. J. Am. Chem. Soc. 138 (27), 8569–8580. https://doi.org/10.1021/jacs.6b04372.

Ruslan, R.K., Sergey, V.K., Yuliya, S.R., Albina Yu.Z., Irek R.N., Marsil K.K., Shamil K.L, Lucia Ya.Z., 2018. Supramolecular assemblies involving calix[4]resorcinol and surfactant with pH-induced morphology transition for drug encapsulation. J. Mol. Liq. 261, 218–224. https://doi.org/10.1016/j.molliq.2018.04.018

Ruslan, R.K., Yuliya S.R., Albina, Y.Z., Rezeda K.M., Anastasiya S. S., Alexandra D.V., Irek, R.N., Marsil K.K., Lucia Ya.Z., 2020. Design of *N*-Methyl-D-glucamine- based resorcin[4]arene nanoparticles for enhanced apoptosis effects. Mol. Pharmaceutics. 17(1), 40–49. https://doi.org/10.1021/acs.molpharmaceut.9b00599

Ruslan, K., Yuliya, R., Albina, Z., Tatiana, S., Nadezda, K., Anastasiia, S., Alexandra, V., Irek, N., Vadim, S., Lucia, Z., 2020. Supramolecular assembly of calix[4]resorcinarenes and chitosan for the design of drug nanocontainers with selective effects on diseased cells. New J. Chem. 44, 17854–17863. https://doi.org/10.1039/D0NJ02163F.

Rustem, A., Zuleykha, M., Asiya, M., Irina, C., Svetlana, S., Igor, A., Alexander, K., 2005. A first report on ternary complex formation between *p*-sulfonatothiacalix[4]arene, tetramethylammonium ion and gadolinium (III) ion in aqueous solutions. Inorg. Chem. Commun. 8, 821–824. https://doi.org/10.1016/j.inoche.2005.06.010.

Sayed, Z.M., Tayebeh, S., Daryoush, A., Mohammad, A.T., Yar, M. B., 2016. Applicability of cloud point extraction for the separation trace amount of lead ion in environmental and biological samples prior to determination by flame atomic absorption spectrometry. Arab. J. Chem. 9, S610–S615. https://doi.org/10.1016/j.arabjc.2011.07.003.

Shalaeva, Ya.V., Morozova, J.E., Ermakova, A.M., Nizameev, I.R., Kadirov, M.K., Kazakova, E.Kh., Konovalovet A.I. 2017. One-step synthesis of gold colloids using amidoaminocalix[4] resorcinarenes as reducing and stabilizing agents. investigation of naproxen binding. Colloid. Surf. A 527, 1–10. https://doi.org/10.1016/j.colsurfa.2017.04.079

Silva, E.L., Roldan, P.S., 2009. Simultaneous flow injection preconcentration of lead and cadmium using cloud point extraction and

determination by atomic absorption spectrometry. J. Hazard. Mater. 161, 142–147. https://doi.org/10.1016/j.jhazmat.2008.03.100.

Sounderajan, S., Kuma,r G.K., Udas, A.C., 2010. Cloud point extraction and electrothermal atomic absorption spectrometry of Se (IV)− 3,3'-Diaminobenzidine for the estimation of trace amounts of Se (IV) and Se(VI) in environmental water samples and total selenium in animal blood and fish tissue samples. J. Hazard. Mater. 2010, 175, 666−672. https://doi.org/10.1016/j.jhazmat.2009.10.061

Souz, E.J.d.S., Amaral, C.D.B.d., Nagata, N., Grassi, M.T., 2020. Cloud point extractors for simultaneous determination of Pd and Pt in water samples by ICP OES with multivariate optimisation. Microchem. J. 152, 104309. https://doi.org/10.1016/j.microc.2019.104309

Su, K., Wang, W., Li, B., Yuan, D., 2018. Azo-bridged Calix[4]resorcinarene-based porous organic frameworks with highly efficient enrichment of volatile iodine. ACS Sustain. Chem. Eng. 6 (12), 17402–17409. https://doi.org/10.1021/acssuschemeng.8b05203.

Thongsaw, A., Sananmuang, R., Udnan, Y., Ross, G.M., 2019. Dual-cloud point extraction for speciation of mercury in water and fish samples by electrothermal atomic absorption spectrometry. Spectrochim. Acta B 160,. https://doi.org/10.1016/j.sab.2019.105685 105685.

Timmerman, P., Verboom, W., Reinhoudt, D.N., 1996. Resorcinarenes. Tetrahedron 52 (8), 2663–2704. https://doi.org/10.1016/0040-4020(95)00984-1.

Twum, K., Rautiainen, J.M., Yu, S., Truong, K.-N., Feder, J., Rissanen, K., Puttreddy, R., Beyeh, N.K., 2020. Host-guest Interactions of sodiumsulfonatomethyleneresorcinarene and quaternary ammonium halides: an experimental-computational analysis of the guest inclusion properties. Cryst. Growth Des. 20, 2367–2376. https://doi.org/10.1021/acs.cgd.9b01540.

Ulusoy, H.İ., Gürkan, R., Ulusoy, S., 2012. Cloud point extraction and spectrophotometric determination of mercury species at trace levels in environmental samples. Talanta 88, 516–523. https://doi.org/10.1016/j.talanta.2011.11.026.

Wei, Y., Li, Y., Quan, X., Liao, W., 2010. Cloud point extraction and separation of copper and lanthanoids using Triton X-100 with water-soluble p-sulfonatocalix[4]arene as a chelating agent. Microchim. Acta 169, 297–301. https://doi.org/10.1007/s00604-010-0353-x.

Wen, X., Deng, Q., Ji, S., Yang, S., Peng, L.i., 2012. Design of rapidly synergistic cloud point extraction of ultra-trace lead combined with flame atomic absorption spectrometry determination. Microchem. J. 100, 1–35. https://doi.org/10.1016/j.microc.2011.08.005.

Yamanaka, M., Kawaharada, M., Nito, Y., Takaya, H., Kobayashi, K., 2011. Structural alteration of hybrid supramolecular capsule induced by guest encapsulation. J. Am. Chem. Soc. 133 (41), 16650–16656. https://doi.org/10.1021/ja207092c.

Zairov, R.R., Elistratova, Y.G., Mustafina, A.R., Amirova, R.R., Pilishkinab, L.M., Antipina, I.S., Konovalov, A.I., 2009. Extraction of lanthanum and gadolinium(III) at the cloud point using p-sulfonatocalyx[n]arenes as chelating agents. Colloid J. 71, 69–75. https://doi.org/10.1134/S1061933X09010086.

Zhang, Z., Li, L., An, D., Li, H., Zhang, X., 2020. Triazine-based covalent organic polycalix[4]arenes for highly efficient and reversible iodine capture in water. J. Mater. Sci. 55, 1854–1864. https://doi.org/10.1007/s10853-019-04164-6.

Zhao, L., Zhong, S., Fang, K., Qian, Z., Chen, J., 2012. Determination of cadmium(II), cobalt(II), nickel(II), lead(II), zinc(II), and copper(II) in water samples using dual-cloud point extraction and inductively coupled plasma emission spectrometry. J. Hazard. Mater. 239–240, 206–212. https://doi.org/10.1016/j.jhazmat.2012.08.066.